Break-up Time in Inkjet Printing from Bulk Rheological Data

Maik Müller[1], Gustaf Mårtensson[2], Ingo Reinhold[1], Tim Wickens[3], Werner Zapka[1]; [1] XaarJet AB, Järfälla, Sweden, [2] Mycronic AB, Täby, Sweden, [3] Xaar plc, Cambridge, UK

Abstract

A number of mathematical methods exist to characterize the underlying mechanism of the thinning and break-up of a liquid jet. These methods however, have not been applied to fluids used in inkjet printing. In this work, we used filament stretching experiments to demonstrate the applicability of similarity solutions found in literature to determine the dominating thinning mechanism for a variety of sample fluids. The thinning velocities and break-up times were computed and compered with the experimental results from the filament stretching. We observed that an additional correction factor was required to match the used similarity solutions with the experimental data. Furthermore, we could calculate the break-up time of the filament experiment from the bulk data of the sample fluids. The calculation was used to predict the overall break-up time of a liquid jet emerging from the nozzle of an inkjet printhead. The results were in good agreement with the general limits of drop formation. Differences between the required pre-factors and from literature were observed and need to be investigated further.

Introduction

The interest in inkjet printing as a manufacturing technique beyond graphical applications is increasing steadily. Its unique features, such as a non-contact, low volume, additive process, combined with the possibility of a dynamic pattern change and deposition of a variety of fluids, open many new fields of applications. Such areas include among others, electronic and display manufacturing or biological applications. These applications require fluids with specific properties, such as metal nanoparticles or functional polymers, and may introduce a different rheological behavior compared to graphical inks. For the development of suitable processes and improved inkjet technologies, a general understanding of the drop formation and related fluid and flow properties is required.

Generally, two approaches to describe the fluid and flow properties can be identified. On the one hand, a variety of mathematical models were proposed that describe fundamental drop formation of Newtonian [1] and non-Newtonian fluids [2] or inkjet related drop formation discussing polymeric [3] and elastic properties [4]. On the other hand, similarity solutions derived from fundamental investigations in fluid mechanics can be applied to droplet formation in a dripping or jetting mode for a variety of fluids of various properties [5]. However, these publications do not necessarily discuss the application within inkjet printing. Furthermore, current evaluation methods of jetability require large fluid volumes which are not available in the field of advanced applications due to the high costs of the materials of interest.

In this work, we present an approach to utilize existing similarity solutions for thinning velocities and break-up times that may be applied to inkjet fluids. The respective equations will be briefly presented. Sample fluids with different additives, such as a surfactant, a dispersant and nanoparticles were used to assess their thinning properties with a filament stretching experiment. The modeling and experimental results were compared, where the required bulk rheological properties, such as surface tension, density and viscosity, were measured for each sample. The correlations that were found were used to predict the break-up time during drop ejection in an inkjet printhead.

Thinning Profiles and Velocities

The thinning profile from a filament stretching experiment of a fluid can be used to partly characterize its fluidic properties and the physical background of the thinning process. It is the evolution of the radius, R, of the overall ligament, as a function of time as shown at time t_2 in Figure 1. Depending on the observed shape and slope of the thinning, a variety of regimes can be identified which are caused by inertia or viscous effects, a decrease in extensional viscosity or elastic finite extensibility [5].

During the thinning process, transitions between the regimes can occur and due to a possibly poor time resolution at the moment of break-up, it is difficult to distinguish the dominating regimes. It is more useful to compute the thinning velocities at the mid-filament radius, R_{mid}, and distinguish the inertia-, viscosity- and elasticity-controlled regimes.

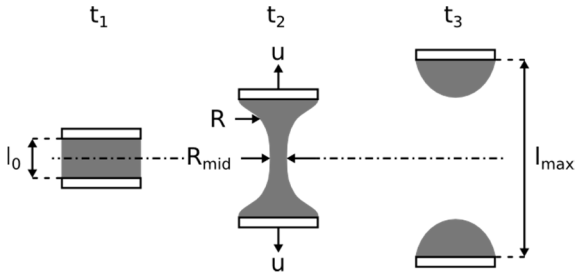

Figure 1. *Principle of extensional rheometry where a fluid element is placed between two plates and an initial distance l_0. The plates move in opposite directions to a maximum distance l_{max} at a constant velocity* u (time t_1 to t_3). *A ligament initiates with a given radius R and thins until break-up, where the mid-filament radius R_{mid} is observed.*

The thinning velocity is the rate at which the ligament radius reduces until break-up into two separate fluid reservoirs attached to the plates (cf. t_1 to t_3 in Figure 1). It is assumed to be similar to a fluidic jet leaving the nozzle of a printhead where multiple effects contribute to the break-up and separation of a liquid filament into a droplet. The thinning is related to capillary effects and can be associated with the capillary velocity, u_{cap}, such that

$$u_{cap} = -\frac{dR}{dt}, \qquad (1)$$

where u_{cap} has to be larger than the velocity of the jet for a successful break-up. The thinning depends on the capillary pressure, p_{cap}, which is a function of the curvature of the ligament, $1/R$, and the surface tension, γ, such that

$$p_{cap} = \frac{\gamma}{R}. \quad (2)$$

However, the fluid properties viscosity, inertia and elasticity oppose the capillary thinning. The dominating force can be balanced with the capillary pressure in order to identify the dominating regime as described below. The description below is a summary of [5] due to the scope of this article.

Viscosity-controlled Thinning

For the case of large viscosities, the thinning process is balanced by the viscous stress, σ, which can be written as

$$\sigma = 3\eta\dot{\varepsilon}, \quad (3)$$

where η is the viscosity of the fluid and extension rate, $\dot{\varepsilon}$, as

$$\dot{\varepsilon} = -\frac{2}{R}\frac{dR}{dt}, \quad (4)$$

with the ligament radius, R, and the time, t. If the ligament is assumed to be axis-symmetric, the force balance, combining (2) to (4), can be written as

$$\frac{\gamma}{R} = 3\eta\left(-\frac{2}{R}\frac{dR}{dt}\right). \quad (5)$$

The term dR/dt can be considered from (1) as the viscous thinning velocity u_η. Simplifying (5) yields

$$u_\eta = \frac{1}{6}\frac{\gamma}{\eta} \approx 0.1666\frac{\gamma}{\eta}, \quad (6)$$

showing that the viscous thinning is independent of the ligament radius. The consideration of a non-cylindrical ligament showed that the liquid thread thins in a self-similar way with a smaller pre-factor compared to 0.1666 in (6) as

$$u_\eta = 0.0709\frac{\gamma}{\eta}. \quad (7)$$

Similar to the velocity, the filament lifetime or break-up time, t_η, can be computed as

$$t_\eta = 14.1\frac{\eta R_0}{\gamma}, \quad (8)$$

where R_0 is the initial radius of the filament.

An alternative, smaller pre-factor of 0.0304 for (7) and 32.89 in (8) was proposed by *Eggers* and presented by *Clasen et al.* [5] for an asymmetric solution at very thin filament radii, where velocities in the filament become so large that inertia effects cannot be neglected.

Inertia-controlled Thinning

If the viscosity is low enough, capillary thinning is balanced by the inertia of the fluid. The solution depends, in contrast to the viscous thinning, on the filament radius and can be written as

$$u_\rho = 0.3413\sqrt{\frac{\gamma}{\rho R}}, \quad (9)$$

where ρ is the density of the fluid. The moment of break-up can be calculated using

$$t_\rho = 1.9531\frac{\rho R_0^3}{\gamma}. \quad (10)$$

Elasticity-controlled Thinning

In the presence of a visco-elastic fluid, elasticity may oppose the capillary thinning. The measure of visco-elasticity is the longest relaxation time, λ. The extension rate, $\dot{\varepsilon}$, for such a fluid is only dependent on the relaxation time as

$$\dot{\varepsilon} = \frac{1}{\lambda}. \quad (11)$$

The elasticity-controlled thinning velocity can then be computed as

$$u_\lambda = \frac{1}{3}\frac{R}{\lambda}, \quad (12)$$

showing that the thinning velocity is dependent neither on the viscosity, nor the surface tension of the fluid.

Experimental

To investigate a possible application of the presented similarity solutions to fluids used in inkjet, three sample fluid series were prepared. For two series, the monomer Propoxylated (2) neopentyl glycol dyacrylate (PONPGDA) was used and its properties were altered by adding either a surfactant (< 1,000 gmol^{-1}) or dispersant (< 100,000 gmol^{-1}). The nominal mass concentrations of the additives were measured with a balance (PB303-S, Mettler Toledo, Switzerland). After the additives were added at room temperature, the samples were shaken for 15 min to ensure a homogenous mixture. A blank sample of pure PONPGDA was prepared to serve as reference.

The third series was prepared using a silver metal nanoparticle (MNP) ink where the ink's solvent was evaporated to achieve a decrease in solvent concentration. Therefore, the samples were placed on a hot plate at 65 °C while the weight was monitored every 30 min to evaluate the relative change in weight and hence the nominal mass of evaporated solvent. The respective concentrations of the samples are denoted in Table 1. The reference sample for this series was the original MNP ink where no solvent was evaporated.

Surface tension, density and viscosity values required for the computation of the similarity solutions were measured separately.

Table 1. Concentrations of prepared samples.

Sample Series	Concentration of additive or evaporated solvent (wt%)
Blank	0
Dispersant	0.1, 0.5, 1, 2.5, 5, 10
Surfactant	0.1, 0.25, 0.5, 1, 5
MNP	0, 5, 10, 15

The filament stretching experiments were performed using the *TriMaster MKII*. The setup consisted of a continuous light source, high-speed camera and conveyor belt that carried two pistons that represent the two plates shown in Figure 1. The radius of the pistons was 600 µm. The experiment was conducted at 20 °C. The samples could not be heated to ensure similar viscosities of the samples. The separation velocity (cf. u in Figure 1) was 75 mms^{-1}. The images for analysis were recorded with 6000 frames per second and the mid-filament radius was evaluated with the provided software *TriVision 1.1*. The samples were applied using a microliter pipette and repeated until straight vertical filament was achieved.

Results and Discussion

Thinning Velocities

The thinning velocity was computed using the mid-filament radius R_{mid} from the filament stretching experiment as

$$u = -\frac{dR_{mid}}{dt},$$

where an example for the dispersant with 5 wt% concentration is depicted Figure 2. The characteristic velocities shown in Equation (6), (7) and (9) were computed and added to Figure 2. The Eggers pre-factor of 0.0304 was used to calculate u_η as it was found to match all fluids with a viscosity of 20 mPa s at the measurement temperature of 20 °C.

A mismatch of the characteristic velocities was observed for samples with a larger or smaller viscosity than 20 mPa s at 20 °C. The sample shown in Figure 2 had a viscosity of approximately 29 mPa s at the measurement temperature. In order to match the experimental data, an additional correction factor was introduced for every investigated sample. It was found that the factor scaled linearly with the viscosity of the samples at the measurement temperature as shown in Figure 3 for the calculation of u_η. Adding the correction factor matched the characteristic velocity with the experimental data as shown in Figure 2.

Similar deviations were found for the inertia-controlled thinning velocity, u_ρ, where a similar correction was introduced which decreased linearly with increasing viscosity at measurement temperature as shown in Figure 4. This correction factor was considered for a corrected calculation of u_ρ in Figure 2 and the result matched the experimentally observed velocity.

The relaxation time, λ, could not be measured and was manually evaluated that the slope of Equation (12) matched with the experimental data. The respective value for λ was at a constant value of 115 µs for the surfactant and dispersant sample series and decreased from 300 to 100 µs for increasing concentrations of the MNP series. The match of the elasticity-controlled thinning velocity, u_λ, is shown in Figure 2. The matched relaxation times were rather large and it was doubtful that the value did not change for the dispersant samples as the added polymer was expected to change the relaxation time. Therefore, the values should be considered as incorrect and will be not considered in the following.

From the comparison of the experimental and computational data it could be observed that the thinning of the ligament could be divided into different dominating regimes that are shown in Figure 2. Initially, after the pistons started their movement, the thinning velocity increased to a value representing the viscosity-controlled thinning within 2 ms. This velocity was kept for 8 ms. Within a short time at the end of the thinning process, the velocity increased to a maximum related to u_ρ within 0.5 ms. Once the maximum was reached, the velocity dropped within another 0.5 ms which could be related to u_η. The two regimes before break-up differed between the samples and significantly for the samples with large concentrations, such as, the 10 wt% dispersant and the 15 wt% MNP sample indicating a change in dominating properties.

The observed additional correction factor was not discussed by *Clasen et al.* [5]. They used larger viscosities beyond 1 Pa s and it appeared from the presented results that the additional correction was required for viscosities smaller than 100 mPa s.

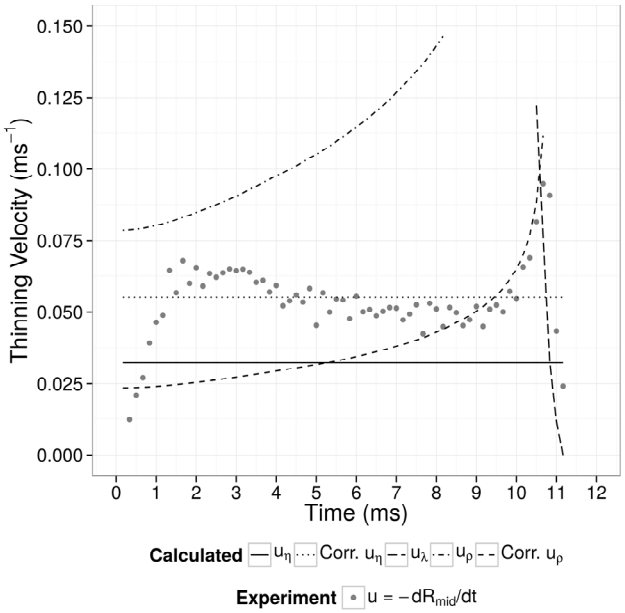

Figure 2. *Example of experimental and computed thinning velocity of a filament stretching experiment (dispersant sample with 5 wt% loading).*

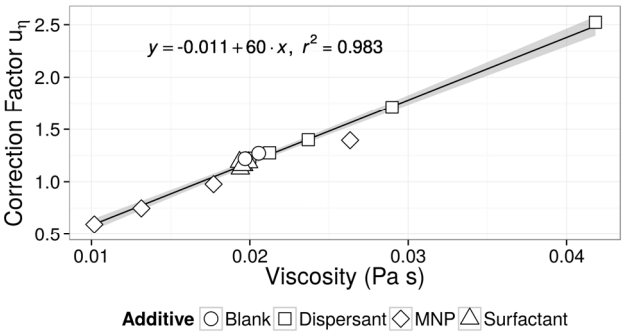

Figure 3. *Correction factor for viscosity-controlled thinning velocity, u_η, as a function of viscosity, η.The fitting was performed with a linear model shown as a solid line. The standard deviation is shown as the surrounding grey area.*

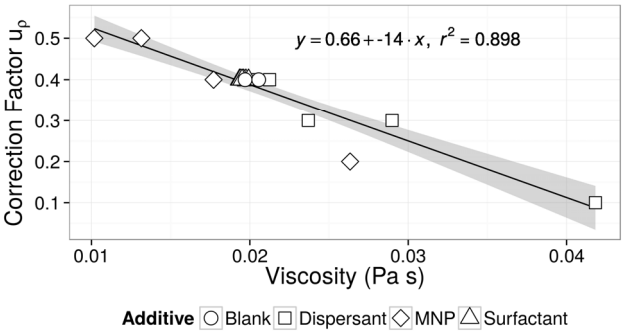

Figure 4. *Correction factor for inertia-controlled thinning velocity, u_ρ, as a function of viscosity, η. The fitting was performed with a linear model shown as a solid line. The standard deviation is shown as the surrounding grey area.*

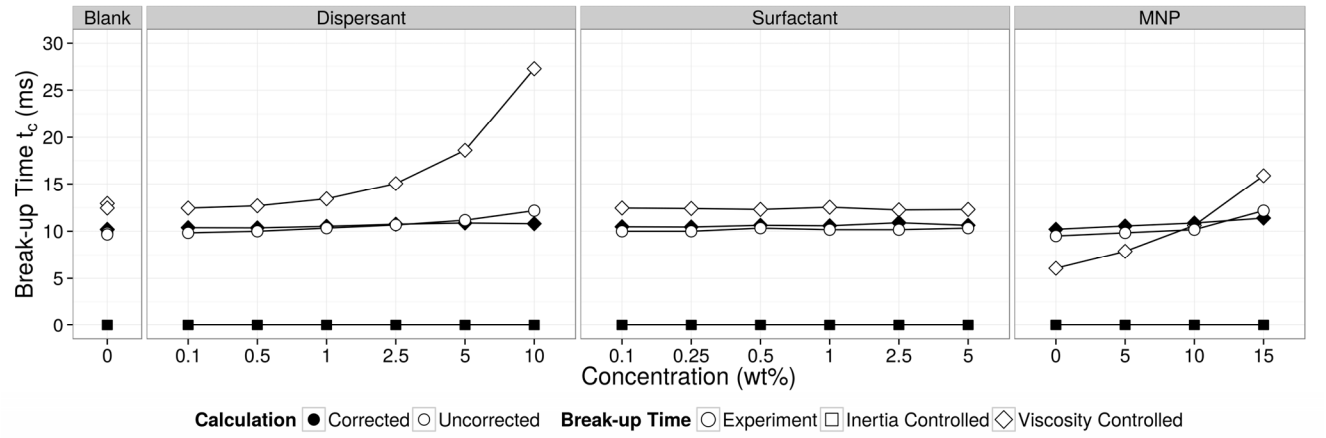

Figure 5. *Experimental and computed break-up times of all sample fluids of the filament stretching experiment. Both the results with the corrected and original pre-factors are shown.*

With the provided similarity solutions, the thinning velocities could be estimated from the bulk data only. However, due to the uncertainty of the corrections of λ and u_λ, it was not considered in the subsequent discussion. Furthermore, the experiment should be repeated, as well as extended, using a complete set of measured physical properties at the required temperatures.

Experimental Break-up Time

The characteristic break-up time of a filament can be calculated using Equations (8) and (10). The elasticity-controlled break-up time was not considered as λ was not measured. In order to compute the break-up times, the required initial radius, R_0, was set to the radius of the pistons of the *TriMaster* of 600 µm. The experimental data and the computation results are shown in Figure 5, where the Eggers factor was used for the viscosity-controlled break-up time since it was within the range of the experimental observation. Therefore, Equation (8) becomes

$$t_\eta = 32.89\frac{\eta R_0}{\gamma}.$$

The inertia-controlled break-up time was very small with values close to zero, which was related to size of the pistons and the scaling by R_0^3. From this, it was concluded that the thinning behavior was not dominated by inertial effect, which was in agreement with the computation of the thinning velocity as shown in Figure 2, where the viscosity-controlled thinning covers most of the thinning time.

In contrast, the break-up time controlled by viscous forces, t_η, agreed with the experimental data if the right correction factor was used as shown in Figure 5. Using the unmodified Eggers factor it, was found that the computed break-up times were close to the experimental data, but still larger. Applying the observed correction factor for each fluid (cf. Figure 3) showed that the experimental data could be matched.

The results showed that the thinning behavior was mainly viscosity controlled, which is in agreement with the data from the computation of the thinning velocities. Furthermore, it was an indication of a possible requirement of an additional correction of the Eggers pre-factor for low viscosities. However, it should be considered that the surface tension and density were not measured at the temperature of the filament-stretching experiment and this could introduce a certain error.

Prediction of Break-up Time in Jetting

Since the computation of the break-up times was independent of the evolving mid-filament radius, the radius could be used to calculate the possible break-up time of a liquid jet in an inkjet printhead. As an example, a *Xaar126/50* printhead with a nominal drop volume of 50 pL and a nozzle diameter of 40 µm was considered.

In order to locate the possible position of break-up during jetting, the actual travel distance of a drop from the nozzle at a certain time was calculated using

$$t = \frac{s}{v}, \tag{13}$$

where the velocity, v, was chosen as 6 ms^{-1}, which is a typical velocity for droplets emitted from this printhead. The travel time, t, was calculated for distances, s, not larger than 1000 µm as typical distance of nozzle plate and substrate. The maximum travel time to reach 1000 µm was calculated as 166 µs. The distances are depicted as dashed lines in Figure 6, where the respective distances are annotated.

The inertia-controlled break-up time was close to zero and similar to the filament experiment. The viscous-controlled break-up time was calculated with a variety of pre-factors as shown in Figure 6. If the Eggers factor (32.89) was used, the break-up would have occurred at 220 µs, which was larger than the maximal distance to the substrate. Using the additional correction factor for viscosities of 10 mPa s from Figure 3 gives an additional pre-factor of 0.59 (total pre-factor was 19.0247) resulted in a possible break-up after 125 µs, i.e. between 700 and 800 µm from the nozzle, which is unrealistically far from the nozzle.

If the unmodified standard pre-factor (14.1) was used, the break-up would occur at approximately 600 µm. This was a reasonable result if the break-up time is considered as the time of

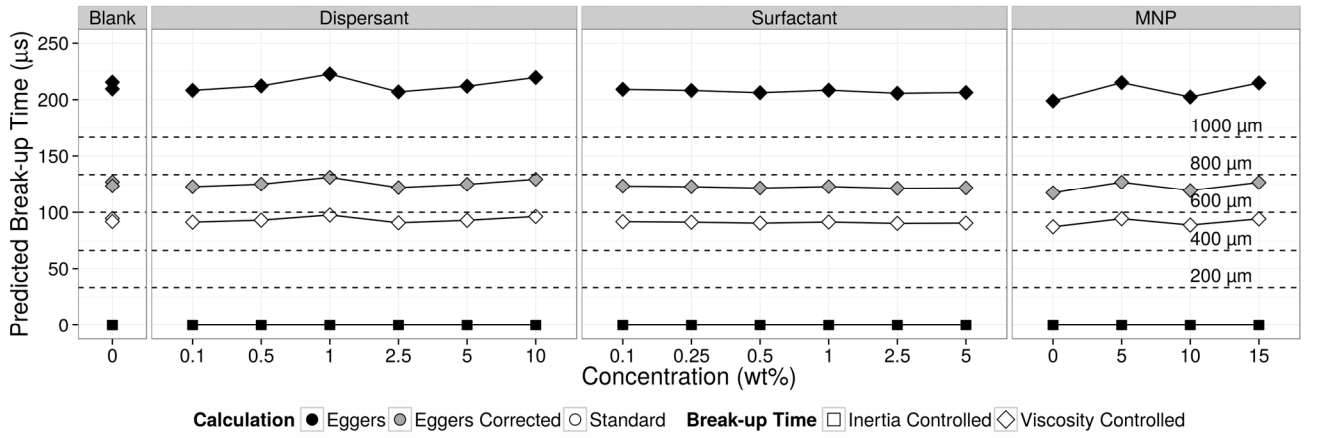

Figure 6. *Predicted, possible break-up time of the main droplet in an inkjet printhead (Xaar126/50) considering the bulk properties of the sample fluids. A variety of pre-factors were used to determine the most appropriate calculation.*

travel of the leading drop until the ligament or tail broke up from the connection to the meniscus at the nozzle. During flight, the ligament extends between the nozzle and the leading droplet. The ligament detaches if surface tension forces overcome the viscous or capillary forces. Until this detachment, the leading drop has travelled a certain distance which could be the calculated viscosity-controlled break-up time, t_η. Therefore, t_η could be considered as the maximum travel distance or the time at which the droplet detached from the nozzle and meniscus, respectively. This calculation could provide an estimation of the actual time-scale in which the detachment from the nozzle occurs.

However, to validate the calculation and evaluate the correct pre-factor, further measurements and calculations of a larger variety of samples and sample configurations have to be performed. Additionally, the actual break-up time should be determined from a jetting experiment.

Conclusions

In this work, we introduced the similarity solutions for the thinning velocity and break-up time of a liquid filament found in the literature for the use with inkjet fluids. We used a collection of sample fluids to apply the solutions to the experimental observation from filament stretching experiments. We observed that an additional correction factor was required to match the calculations with the experimental data. We found that the factor was a function of the viscosity of the sample fluids at the measurement temperature of the filament experiment. From this, break-up times that required only the bulk rheological data of the fluid were computed. It was found that the break-up time of the filament experiment could be successfully matched. The similarity solutions and calculation of the additional correction factor were adopted for the geometries of an inkjet printhead showing that the computed break-up time of a droplet emerging from the nozzle of a printhead results in reasonable timings. In addition to this, it was found that the underlying mechanism was related to viscous forces.

Such a calculation could be used to determine the general mechanisms and break-up time of inkjet fluids prior to jetting with the advantage of using only small fluid quantities to determine the required bulk rheological data. However, further experiments with an exact set of bulk data at the respective measurement temperatures are required to validate the observed correction factors and most suitable pre-factor for inkjet fluids. Furthermore, the relaxation time should be measured to include the elasticity-controlled thinning and the actual break-up time of a droplet from an inkjet printhead should be determined.

Acknowledgement

We would like to thank Simon Butler from the *Department of Chemical Engineering* at *Cambridge University* for his support and guidance during the filament stretching experiments.

References

[1] J. Eggers, E. Villermaux (2008). Physics of liquid jets. Reports on Progress in Physics, 71(3), 036601.

[2] M. Ochowiak, S. Woziwodzki (2007). The break-up of jet in non-Newtonian systems. In Proceedings of European Congress of Chemical Engineering (ECCE-6).

[3] S. D. Hoath, I.M. Hutchings, G. D. Martin, T. R. Tuladhar, M. R. Mackley, D. Vadillo (2009). Links Between Ink Rheology, Drop-on-Demand Jet Formation, and Printability. Journal of Imaging Science and Technology, 53(4), 041208.

[4] N. F. Morrison, O. G. Harlen (2010). Viscoelasticity in inkjet printing. Rheologica Acta, 49(6), 619–632.

[5] C. Clasen, P. M. Phillips, L. Palangetic, J. Vermant (2012). Dispensing of rheologically complex fluids: The map of misery. AIChE Journal, 58(10), 3242–3255.

Author Biography

Maik Müller received his bachelor degree in Media Production from Chemnitz University of Technology, Germany, where he focused on inkjet printing of conductive materials. He continued his studies as master student in Fluid Mechanics at the Royal Institute of Technology (KTH) in Stockholm, Sweden and Xaar's Advanced Application Technology group in Järfälla, Sweden. During his Master's, he focused on the rheological characterization of complex fluids and jetability in inkjet printing and continues as a member of Xaar's Advanced Application Technology group.